Proactive Collision Avoidance for ASVs using A Dynamic Reciprocal Velocity Obstacles Method*

D. K. M. Kufoalor, E. F. Brekke, and T. A. Johansen

***Abstract*— We propose a collision avoidance method that incorporates the interactive behavior of agents and is proactive in dealing with the uncertainty of the future behavior of obstacles. The proposed method considers interactions that will be experienced by an autonomous surface vessel (ASV) in an environment governed by the international regulations for preventing collisions at sea (COLREGs). Our approach aims at encouraging dynamic obstacles to cooperate according to COLREGs. Therefore, we propose a strategy for assessing the cooperative behavior of obstacles, and the result of the assessment is used to adapt collision avoidance decisions within the Reciprocal Velocity Obstacles (RVO) framework. Moreover, we propose a predictive approach to solving known limitations of the RVO framework, and we present computationally feasible extensions that enable the use of complex dynamic models and objectives suitable for ASVs. We demonstrate the performance and potentials of our method through a simulation study, and the results show that the proposed method leads to proactive and more predictable ASV behavior compared with both Velocity Obstacles (VO) and RVO, especially when obstacles cooperate by following COLREGs.**

I. Introduction

The international regulations for preventing collisions at sea (COLREGs) [1] require actions made to avoid collision to be first *proactive*, and if necessary, *reactive* (see [1] Rule 8, and [2]). Proactive decisions are deliberate and clear decisions, intended to control a *situation* rather than just responding to it after it has happened.

However, most existing collision avoidance approaches tend to be more reactive, instead of proactive, probably due to the lack of effective strategies for handling the uncertainty associated with the future behavior of dynamic obstacles. A related issue is that a reactive situation may occur when the decision making process fails to consider the possible effect of the decision on the future behavior of other agents. Moreover, several results in the literature show that, if the interaction between agents are considered, we can enhance collision avoidance decisions (see e.g. [3], [4]).

While existing reciprocal collision avoidance methods expect dynamic obstacles to share the responsibility for collision avoidance *equally*, more general approaches (e.g. reflective navigation [4]) consider the behavior of obstacles at different reasoning levels. However, for such reflective approaches to be practically feasible, one has to assume a fixed level of intelligence for the obstacles and deal with the associated uncertainties in a reactive manner.

The Velocity Obstacles (VO) method is a well-established collision avoidance method that applies relative motion arguments to achieve collision avoidance maneuvers. Although the original VO method [5] is reactive and may produce decisions that are not feasible for relatively slow applications like marine vessels with dynamic constraints, some proposals in the literature (e.g. [6], [7]) incorporate the agent's dynamics in the VO method either by formulating the VO problem in the agent's control input space or some other appropriate state-dependent configuration space. Moreover, the results of [7] show that choosing the agent's target velocity as a high-level control input, and consequently abstracting the low-level control inputs, is probably the most practical approach when considering a heterogeneous dynamic environment.

In general, we find the VO method as a convenient framework (i.e. simple, easy to adapt and tune) for strategic proactive COLREGs-compliant decision making, compared with other known collision-avoidance methods such as Dynamic Window (DW) [8], Inevitable Collision States (ICS) [9], and some MPC approaches [10], [11]. In fact, different existing variations of the VO method, such as Reciprocal Velocity Obstacles (RVO) [3], Hybrid RVO [12], and Probabilistic VO [4] approaches, have strategic elements that can be used in proactive decision making.

For the above reasons, we derive a proactive collision avoidance method for ASVs using the VO framework, and the main contributions include a strategy for adapting the predicted share of responsibility w.r.t. dynamic obstacles, predictive feasible decision making, and COLREGs-compliance.

II. Velocity obstacles framework

In this section, we introduce the notations, definitions, and properties of the VO framework, which facilitate the design of a dynamic reciprocal velocity obstacles (DRVO) method.

A. Safe passage circle and closest point of approach

The agents in this work are considered to be circular-shaped (planar) dynamic objects whose boundaries describe safety zones typically defined around marine vessels. For collision avoidance decisions made from a long range, which depends on the type of obstacle, environment etc, it is common practice to specify a minimum separation distance at the closest point of approach (CPA) to the obstacle (see e.g. [13]). We denote the radius of the ASV, represented by agent A, as $r_A > L_A/2$, where L_A is the length of the ASV,

All authors are with the Center for Autonomous Marine Operations and Systems (AMOS), Department of Engineering Cybernetics, Norwegian University of Science and Technology (NTNU), O.S. Bragstads plass 2D N-7491 Trondheim, Norway. {kwame.kufoalor, edmund.brekke, tor.arne.johansen}@ntnu.no

* This work was supported by the Research Council of Norway (NFR) through the projects 223254 and 244116/O70. The professorship of the Edmund Brekke is funded by DNV GL.

and we define the radius of the safe passage circle around an obstacle vessel B of length L_B as $r_B := d_{AB}^{min} - r_A > L_B/2$. The distance d_{AB}^{min} is the desired minimum distance between the ASV and obstacle B at CPA (i.e. d_{AB}^{CPA}). Hence,

$$d_{AB}^{\text{CPA}} \geq d_{AB}^{min} \tag{1}$$

implies that the ASV does not collide with obstacle B.

Let $\mathbf{v}_{A|B} = \mathbf{v}_A - \mathbf{v}_B$, and $\mathbf{p}_{BA} = \mathbf{p}_B - \mathbf{p}_A$. We denote the time to CPA by t_{AB}^{CPA}, which is computed by assuming both vessels keep their velocities, $\mathbf{v}_A$ and $\mathbf{v}_B$, constant. Specifically, we find the time at which the distance between A and B is minimum by solving for t in $\frac{\partial}{\partial t}\|(\mathbf{p}_A + t\,\mathbf{v}_A) - (\mathbf{p}_B + t\,\mathbf{v}_B)\| = 0$, which leads to

$$t_{AB}^{\text{CPA}} = \begin{cases} \dfrac{\mathbf{p}_{BA} \cdot \mathbf{v}_{A|B}}{\|\mathbf{v}_{A|B}\|^2} & \text{if } \|\mathbf{v}_{A|B}\| > 0 \\ 0 & \text{otherwise} \end{cases} \tag{2}$$

where $\mathbf{p}_A$ and $\mathbf{p}_B$ are the position vectors of vessel A and B, respectively. Consequently,

$$d_{AB}^{\text{CPA}} = \|(\mathbf{p}_A + t_{AB}^{\text{CPA}}\,\mathbf{v}_A) - (\mathbf{p}_B + t_{AB}^{\text{CPA}}\,\mathbf{v}_B)\|. \tag{3}$$

B. Velocity obstacles

Let $\mathcal{A} \oplus \mathcal{B} = \{\mathbf{a} + \mathbf{b} \mid \mathbf{a} \in \mathcal{A}, \mathbf{b} \in \mathcal{B}\}$ represent the Minkowski sum of the sets $\mathcal{A}$ and $\mathcal{B}$, which describe the shape and size of agents A and B, respectively. Let $-\mathcal{A} = \{-\mathbf{a} \mid \mathbf{a} \in \mathcal{A}\}$ represent the set $\mathcal{A}$ reflected in its reference point, and let $\boldsymbol{\lambda}(\mathbf{p}, \mathbf{v}) = \{\mathbf{p} + t\mathbf{v} \mid t > 0\}$ denote the ray starting at position $\mathbf{p}$ with direction $\mathbf{v}$.

Definition 2.1: (Collision Cone)

$$CC_{A|B} = \{\mathbf{v}_{A|B} \mid \boldsymbol{\lambda}(\mathbf{p}_A, \mathbf{v}_{A|B}) \cap \mathcal{B} \oplus -\mathcal{A} \neq \emptyset\}.$$

The velocity obstacles (VO) method [5] defines a set of velocities, denoted $VO_{A|B}$ for agent A with respect to agent B, that lead to collision in the future, assuming that agent B's velocity is constant over time. Therefore, if it is possible to select agent A's velocity outside $VO_{A|B}$, agent A will not collide with agent B. For the sake of simplicity, we present our VO definitions using the Collision Cone $CC_{A|B}$ that considers the *relative* velocity ($\mathbf{v}_{A|B}$), instead of $VO_{A|B}$, which represents an equivalent condition on the *absolute* velocity, $\mathbf{v}_A$. That is, $VO_{A|B}$ is obtained by translating $CC_{A|B}$ by $\mathbf{v}_B$ as stated in Definition 2.2 (cf. Fig 1a).

Definition 2.2: (Velocity Obstacles)

$$VO_{A|B} = CC_{A|B} \oplus \mathbf{v}_B.$$

When the context is not obvious we specify the current position and velocity as $\mathbf{p}^0$ and $\mathbf{v}^0$, respectively, and $\mathbf{p}^k$, $\mathbf{v}^k$, denote predicted values at prediction point k. The operator $[\cdot]_z$ is used to extract the z component of a cross product, computed using the body-fixed frame where $+x$ points forward, $+y$ points to the right, and $+z$ points downward.

C. Velocity obstacles and closest point of approach

The CPA and VO conditions stated in the previous sections provide different approaches commonly used in making collision avoidance decisions (i.e. using position or velocity space). Due to the constant velocity assumption used in both approaches, choosing a velocity that is not within $VO_{A|B}$ is equivalent to enforcing the d_{AB}^{CPA} condition (1). The following proposition relates the two approaches and specifies properties that allow us to easily use both position and velocity space results in our collision avoidance algorithm.

Proposition 2.1: Consider two point particles A and B moving with constant velocities $\mathbf{v}_A$ and $\mathbf{v}_B$, respectively. Let the radius of the circle centered at $\mathbf{p}_B$ to which the ray $\boldsymbol{\lambda}(\mathbf{p}_A, \mathbf{v}_{A|B})$ is a tangent be denoted by $r\left(\mathbf{p}_B, \boldsymbol{\lambda}(\mathbf{p}_A, \mathbf{v}_{A|B})\right)$. The equivalence of VO and CPA properties can be stated as follows:

(i) The d_{AB}^{CPA} given by (3) using (2) is equal to the radius $r\left(\mathbf{p}_B, \boldsymbol{\lambda}(\mathbf{p}_A, \mathbf{v}_{A|B})\right)$.

(ii) The condition $d_{AB}^{\text{CPA}} = d_{AB}^{min}$ (cf. (1)) is satisfied *iff* $\boldsymbol{\lambda}(\mathbf{p}_A, \mathbf{v}_{A|B})$ is a tangent to the circle with radius $r\left(\mathbf{p}_B, \boldsymbol{\lambda}(\mathbf{p}_A, \mathbf{v}_{A|B})\right) = d_{AB}^{min} > 0$, thus $\boldsymbol{\lambda}(\mathbf{p}_A, \mathbf{v}_{A|B})$ is an edge of the $CC_{A|B}$ specified by $r\left(\mathbf{p}_B, \boldsymbol{\lambda}(\mathbf{p}_A, \mathbf{v}_{A|B})\right)$.

Proof: see Appendix VII-A.

Remark 2.1: For agents that can be represented by circular objects, the center point can be considered as the point particle in Proposition 2.1, and $d_{AB}^{\text{CPA}} = r\left(\mathbf{p}_B, \boldsymbol{\lambda}(\mathbf{p}_A, \mathbf{v}_{A|B})\right)$ must satisfy $r\left(\mathbf{p}_B, \boldsymbol{\lambda}(\mathbf{p}_A, \mathbf{v}_{A|B})\right) \geq d_{AB}^{min} := r_A + r_B$ in order to avoid collision.

As a consequence of Proposition 2.1, we can strategically decrease or increase the CPA by enforcing, respectively, a reduced or expanded collision cone, and vice-versa.

D. Reciprocal velocity obstacles

The reciprocal velocity obstacles (RVO) method [3] introduces the idea of sharing the responsibility for collision avoidance among two agents. Instead of taking full responsibility, as specified by VO, the RVO method suggests that an agent takes only half of the responsibility and assumes that the other agent reciprocates by taking the remaining half. Moreover, RVO in its generalized form may implement any balance in responsibility between two agents as stated in the following definition, and illustrated in Fig. 1b.

Definition 2.3: (Reciprocal Velocity Obstacles)

$$RVO_{A|B}(\alpha_{A|B}) = CC_{A|B} \oplus \big((1 - \alpha_{A|B})\mathbf{v}_A + \alpha_{A|B}\mathbf{v}_B\big).$$

Setting $\alpha_{A|B} = 0.5$ in Definition 2.3 recovers the typical $RVO_{A|B}$ definition, where equal responsibility for mutual collision avoidance is expected from agent A and B.

III. Dynamic Reciprocal Velocity Obstacles

This section presents a DRVO method, which relies on the properties of the VO framework introduced in Section II.

A. DRVO method

The RVO method described in Section II-D was primarily developed to avoid oscillations in a multi-agent navigation task [3], where the assumption that the agents involved are capable of reciprocating each other's effort may be reasonable. However, this assumption is generally not valid, especially when considering a heterogeneous system of agents. Therefore, we propose that an agent adapts its

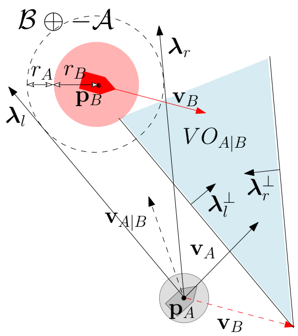

(a) Velocity obstacles (VO): collision cone $CC_{A|B}$ translated by $\mathbf{v}_B$

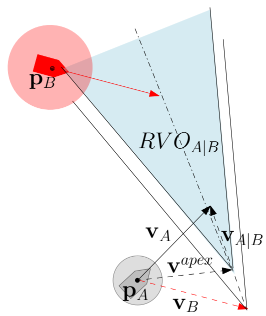

(b) Reciprocal VO: fixed $\mathbf{v}^{apex} = \mathbf{v}_A - \alpha_{A|B}\mathbf{v}_{A|B}$, $\alpha_{A|B} \in (0, 1)$

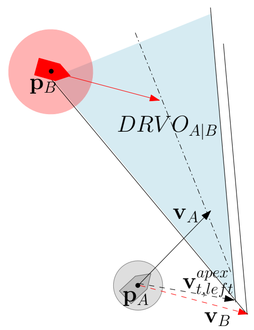

(c) Dynamic RVO: dynamic $\mathbf{v}_{t,left}^{apex}$ with predicted $\alpha_{t,A|B}$

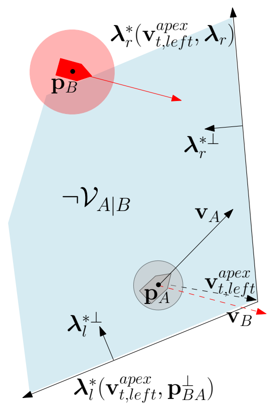

(d) DRVO with COLREGs constraint set $\mathcal{V}_{A|B}$ (in Section III-B)

Fig. 1: Illustration of VO, RVO, DRVO and COLREGs constraints.

share of the collision avoidance responsibility using a time-varying parameter α_t, based on an initial estimate α_0 and an assessment of whether the obstacle is *cooperating* or *not*.

Furthermore, we want the agent to deliberately choose a side to pass an obstacle when a side is not specified by COLREGs (see Fig. 2d). Therefore, we adopt the hybrid idea in [12], where one edge of the resulting DRVO (cone) is obtained from the original VO and the other edge is obtained from the adapted RVO, depending on which side we wish to pass the obstacle (cf. Fig. 1b and 1c). The intersection between the chosen edges form the apex of the DRVO. Specifically, given $\alpha_{t,A|B}$ at time t, we translate the collision cone such that its apex lies at

$$\mathbf{v}_{t,left}^{apex} = \mathbf{v}_B + \frac{(1-\alpha_{t,A|B})\,[\mathbf{v}_{A|B} \times \boldsymbol{\lambda}_r]_z\,\boldsymbol{\lambda}_l}{[\boldsymbol{\lambda}_l \times \boldsymbol{\lambda}_r]_z}, \qquad (4)$$

when B is expected to pass A on its left side, and

$$\mathbf{v}_{t,right}^{apex} = \mathbf{v}_B + \frac{(1-\alpha_{t,A|B})\,[\mathbf{v}_{A|B} \times \boldsymbol{\lambda}_l]_z\,\boldsymbol{\lambda}_r}{[\boldsymbol{\lambda}_l \times \boldsymbol{\lambda}_r]_z}, \qquad (5)$$

when B is expected to pass A on its right side. The specification of the side to pass depends on the COLREGs requirements for the particular situation (treated later in Section III-B). The rays $\boldsymbol{\lambda}_l$, $\boldsymbol{\lambda}_r$ from $\mathbf{p}_A$ are, respectively, the left and right boundaries of $CC_{A|B}$ (see Fig. 1a).

Definition 3.1: (Dynamic Reciprocal Velocity Obstacles) $DRVO_{A|B}(\alpha_{t,A|B}) = CC_{A|B}^* \oplus \mathbf{v}_t^{apex}$, where $\mathbf{v}_t^{apex}$ and the corresponding modified collision cone $CC_{A|B}^*$ are determined using equation (4) or (5).

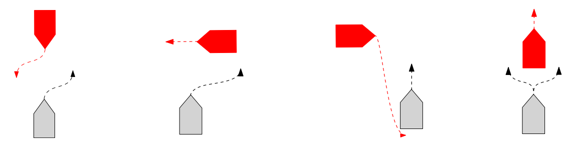

(a) Head-on (b) Crossing from starboard (c) Crossing from port (d) Overtaking

Fig. 2: COLREGs scenarios and actions for two power-driven vessels. The scenarios are described from the gray vessel's perspective.

The parameter $\alpha_{t,A|B}$ is determined by an initial value $\alpha_{0,A|B}$, which is adapted if obstacle B is not cooperating. We adapt $\alpha_{t,A|B}$ towards a predefined limit $\alpha_{t,A|B} = \bar{\alpha}_{t,A|B}$, where $\bar{\alpha}_{t,A|B} = 1$ represents full responsibility. Therefore, $\alpha_{0,A|B}$ is replaced by $\alpha_{-1,A|B}$ (from the previous sampling time) in the following equation, if $\alpha_{-1,A|B} > \alpha_{0,A|B}$.

$$\alpha_{t,A|B} := \begin{cases} \alpha_{0,A|B} & \text{if } \textit{cooperating} \\ \bar{\alpha}_{t,A|B} - \rho_{t,A|B}(\bar{\alpha}_{t,A|B} - \alpha_{0,A|B}) & \text{if } \textit{not cooperating} \end{cases} \qquad (6)$$

where $\rho_{t,A|B} \in (0, 1)$ is a parameter, possibly dependent on t_{AB}^{CPA} and the dynamics of A, which will determine how quickly agent A takes full responsibility to avoid collision with agent B. Note that $\alpha_{0,A|B}$, $\bar{\alpha}_{t,A|B}$, and $\rho_{t,A|B}$ allow different obstacles (and scenarios) to be prioritized differently. We describe an obstacle B as cooperating with agent A if the current motion of B leads to a passage on the side agent A expects it to pass, as specified in the next definition.

Definition 3.2: (Obstacle is cooperating) Agent B is cooperating with agent A if $[\mathbf{v}_{A|B} \times \mathbf{p}_{BA}]_z < 0$, when B is expected to pass on A's left side, or $[\mathbf{v}_{A|B} \times \mathbf{p}_{BA}]_z > 0$, when B is expected to pass on A's right side, and $\mathbf{v}_{A|B}$ may not be collision-free.

When agent A is required to take full responsibility, we use a more strict condition where $\mathbf{v}_{A|B}$ does not lead to collision between agent A and B.

Definition 3.3: (Obstacle is strictly cooperating) Agent B is strictly cooperating with agent A if $[\mathbf{v}_{A|B} \times \boldsymbol{\lambda}_r]_z \leq 0$, when B is expected to pass on A's left side, or $[\mathbf{v}_{A|B} \times \boldsymbol{\lambda}_l]_z \geq 0$, when B is expected to pass on A's right side.

B. DRVO with COLREGs constraints

Some required actions according to COLREGs specify which side to pass an obstacle (see Fig. 2a and 2b). As shown in [13], it is straightforward to include such specifications into a VO framework by considering them as extra constraint sets in the velocity space. For instance, we can specify that vessel A should either stay clear or pass obstacle B while seeing it on the left (or port) side by restricting vessel A's velocity in the COLREGs constraint set (see Fig. 1d):

$$\mathcal{V}_{A|B} = \{\mathbf{v} \mid \mathbf{v} \notin DRVO_{A|B}(\alpha_{t,A|B}),\ [\mathbf{v}_{|B} \times \mathbf{p}_{BA}]_z < 0 \vee [\mathbf{v}_{|B} \times \boldsymbol{\lambda}_l^*(\mathbf{v}_t^{apex}, \mathbf{p}_{BA}^\perp)]_z < 0\}$$

where $\mathbf{v}_{|B} = \mathbf{v} - \mathbf{v}_B$, and $\mathbf{p}^{\perp}_{BA}$ is perpendicular to $\mathbf{p}_{BA}$. The set $\mathcal{V}_{A|B}$ will enforce starboard maneuvers in a head-on or crossing situation (cf. Fig. 2a-2c).

Although we can decide to always choose a starboard maneuver as in [13], we may unnecessarily restrict the vessel's motion in overtaking situations where a port maneuver is the safest choice (cf. Fig. 2d). Therefore, we propose to use only the DRVO constraints in $\mathcal{V}_{A|B}$ when overtaking, and rather choose a velocity that is on the same side of the line bisecting the adapted RVO (cf. Fig. 1b and 1c). This choice also determines which DRVO apex to use in Definition 3.1,

$$\mathbf{v}_t^{apex} := \begin{cases} \mathbf{v}_{t,left}^{apex} & \text{if } \mathcal{V}_{A|B} \text{ applies or } [\mathbf{v}_{A|B} \times \mathbf{p}_{BA}]_z < 0 \\ \mathbf{v}_{t,right}^{apex} & \text{otherwise.} \end{cases} \tag{7}$$

In situations such as crossing from port (left) and when being overtaken, the obstacle is required to take much of the maneuvering responsibility according to COLREGs (cf. Fig. 2c-2d), requiring no extra 'side-specific' constraint on the DRVO. In such cases, using (7) encourages the deliberate choice of side consistent with the side sought by the current velocity (cf. Fig. 1c and 1d).

IV. Predictive Decision Making Using DRVO

After encoding deliberate behavior strategies into the DRVO framework, based on the cooperative behavior of obstacles and required COLREGs actions, it remains to determine the collision avoidance trajectory that best captures the agent's own goals and dynamic limitations. For an ASV (agent A), we propose a collision avoidance trajectory that

- is feasible with respect to the ASV's dynamics,
- minimizes deviations from a preferred velocity $\mathbf{v}_A^{pref}$,
- minimizes changes in velocity, with respect to the last commanded velocity $\mathbf{v}_A^{last}$,
- prioritizes course angle χ and speed v differently, and
- minimizes changes in COLREGs-compliant maneuvers.

Note that the course χ is measured w.r.t. the velocity vector of the ASV and therefore includes an offset between the heading and course angles (see e.g. [14]). In order to arrive at the above goals in a computationally efficient way, we first compute a set Ω_c of candidate feasible velocities with respect to the DRVO and COLREGs constraints, and then we determine a reachable set Ω_r from Ω_c with respect to the ASV dynamics.

A. Feasible velocity candidates

The set of candidate velocities Ω_c is defined as

$$\Omega_c := \Omega_{grid} \cup \Omega_{int} \cup \Omega_{proj}, \tag{8}$$

where Ω_{grid} is a set of velocity grid points (see Fig. 3), which are selected with fixed offsets from $\mathbf{v}_A^{pref}$ and are feasible w.r.t. the constraints,

$$\Omega_0 := \Big\{ \mathbf{v} \mid \mathbf{v} \in \bigcup_{O_j \in \mathcal{O}} \mathcal{V}_{A|O_j},\ \mathcal{O} = \{O_j\}_{j=1}^{n_O} \Big\}, \tag{9}$$

$$|v - v_A| \le a_A^{max} \cdot t_{H_d}, \text{ and } |\chi - \chi_A| \le r_A^{max} \cdot t_{H_d}. \tag{10}$$

The set Ω_0 (9) is the combined COLREGs-constrained DRVO set, considering n_O neighboring obstacles (O_j), and (10) specifies limits on changes in speed v and course χ. The limit a_A^{max} is the max acceleration, r_A^{max} is the max turning rate, and t_{H_d} is the time limit within which a commanded change in velocity should be achieved. The time t_{H_d} is also the horizon used for predicting the ASV's motion from the current velocity $\mathbf{v}_A^0$ to a new velocity (see Section IV-B).

The sets Ω_{int} and Ω_{proj} in (8) are sets of velocities that satisfy (10) and are guaranteed to contain the solution of the following optimization problem,

$$\mathcal{P}_0 := \min_{\mathbf{v} \in \Omega_0} \|\mathbf{v} - \mathbf{v}_A^{pref}\|. \tag{11}$$

The solution to problem $\mathcal{P}_0$ represents the 'ideal' strategic behavior that clearly indicates how the ASV intends to control a particular situation. We therefore include the solution of $\mathcal{P}_0$ in Ω_c to enable the possibility of choosing the 'ideal' strategic behavior for the ASV.

We compute a set of velocities that contains the solution of problem $\mathcal{P}_0$ by exploiting the geometric structure of Ω_0 based on the approach of [15]. Specifically, we consider the set Ω_0 as a union of line segments, which are intersected pairwise. It can be shown (cf. [15], Lemma 1 and 2) that if agent A's preferred velocity $\mathbf{v}_A^{pref}$ lies within Ω_0, the velocity closest to $\mathbf{v}_A^{pref}$ is guaranteed to be in either the set of intersection points (Ω_{int}) that are located on the boundary of Ω_0 or the set of projections (Ω_{proj}) of $\mathbf{v}_A^{pref}$ onto the line segments that describe the boundary of Ω_0.

B. Reachable velocities

We compute the reachable set $\Omega_r \subseteq \Omega_c$ by discarding all velocities in Ω_c that lead to collision during the transition from the current velocity $\mathbf{v}_A^0$ to the candidate velocity. This is necessary since feasibility to Ω_0 assumes instantaneous change in velocity and the future positions may deviate significantly from the DRVO predicted positions (see Fig. 3). The procedure used in computing Ω_r is outlined as follows.

For simplicity's sake, consider an ASV model of the form

$$\dot{\mathbf{x}} = \mathbf{f}(\mathbf{x}, \mathbf{u}, \mathbf{w}), \tag{12}$$

which represents both the kinetic and kinematic equations that describe the ASV's motion (see e.g. [14] for specific models of marine vessels). The vector $\mathbf{x} = (\mathbf{p}, \psi, \mathbf{v}, r)$ represents the state of the ASV, where ψ is the heading, and r is the turning rate. We assume that appropriate transformations between the earth-fixed frame and the body-fixed frame are applied in (12). The vector $\mathbf{w}$ represents the input due to environmental disturbances such as ocean current and wind forces. The vector $\mathbf{u}$ is the control input, which is determined by a control law $\mathbf{u} = \beta(\mathbf{v}^{ref}, \hat{\mathbf{x}}, \hat{\mathbf{w}})$ implemented as an autopilot for tracking the reference velocity $\mathbf{v}^{ref}$, using the estimated state $\hat{\mathbf{x}}$ and disturbances $\hat{\mathbf{w}}$. Consequently, the closed-loop dynamics can be written as

$$\dot{\mathbf{x}} = \mathbf{f}\big(\mathbf{x}, \beta(\mathbf{v}^{ref}, \hat{\mathbf{x}}, \hat{\mathbf{w}}), \mathbf{w}\big). \tag{13}$$

Note that $\mathbf{v}^{ref}$ is typically derived from speed v and course χ references, which may have different priorities. We simulate

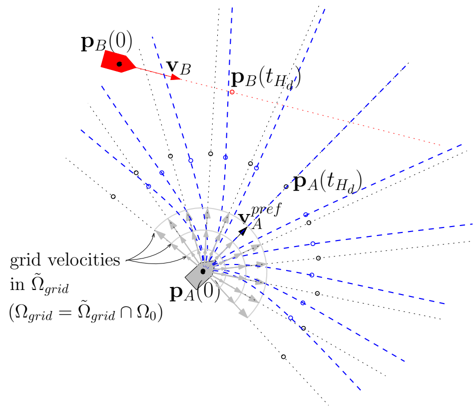

Fig. 3: Example of predictions for candidate velocities (large gray arrows), using a dynamic model (blue, dashed) and straight paths with instant rotation (black, dotted). Predicted positions may differ significantly (e.g. circles at time t_{H_d}). Collision avoidance decisions using CPA or VO arguments may not be valid for time $t < t_{H_d}$, but valid for $t \geq t_{H_d}$ (since predicted trajectories are 'straight lines').

(13) by (numerically) integrating over a relatively short horizon t_{H_d}, using N_d discrete sample times determined by a discretization interval t_s. The simulation of (13), using a candidate $\mathbf{v}^{ref} \in \Omega_c$, provides predicted positions $\{\mathbf{p}_A^k\}_{k=1}^{N_d}$ that are used to compute the predicted distance

$$d_{AO_j}^k = \|\mathbf{p}_A^k - \mathbf{p}_{O_j}^k\| \tag{14}$$

between the ASV (agent A) and each obstacle $O_j \in \mathcal{O}$. We compute $\mathbf{p}_{O_j}^k$ by assuming that the obstacle's motion can be approximated by a straight line trajectory within the time the candidate velocity must be achieved (i.e. t_{H_d}). For a candidate velocity $\mathbf{v}_c$ to be reachable (i.e. $\mathbf{v}_c \in \Omega_r$), it must not lead to collision within time t_{H_d}, and therefore results in predicted distances that are such that

$$d_{AO_j}^k \geq d_{AO_j}^{min}, \ \forall O_j \in \mathcal{O} \text{ and } k \in \{1, 2, \dots, N_d\}. \tag{15}$$

C. Consistent reachable velocities

Finally, we discard reachable velocities, $\mathbf{v}_r \in \Omega_r$, that do not lead to a behavior consistent with the DRVO strategy (i.e. set Ω_0) when reached at time t_{H_d}. That is, we construct $\Omega_{cr} \subseteq \Omega_r$ such that the reachable velocity remains feasible w.r.t. the projection of Ω_0, constructed using predicted positions for time t_{H_d}. Recall that using a VO approach implies that we aim at keeping the ASV's velocity constant when possible. Therefore, we can achieve consistency with Ω_0 by ensuring that, for each obstacle $O_j \in \mathcal{O}$,

$$d^{\text{CPA}}_{AO_j|t_{H_d}}(\mathbf{v}_r) \geq d^{\text{CPA}}_{AO_j|t=0}(\mathbf{v}_r), \text{ for } t^{\text{CPA}}_{AO_j|t_{H_d}} > 0, \tag{16}$$

and the predicted side to pass does not change. Next, we apply a cost function on Ω_{cr} to arrive at a strategic decision.

D. Strategic collision avoidance decision

We select a consistent reachable velocity $\mathbf{v}_{cr} \in \Omega_{cr}$ with speed v and course χ that minimizes the following objective on maneuvering effort and change in behavior:

$$\ell_1(v, \chi; \mathbf{v}_{cr}) = q_v(v - v_A^{pref})^2 + q_\chi(\chi - \chi_A^{pref})^2 + \Delta q_v(v - v_A^{last})^2 + \Delta q_\chi(\chi - \chi_A^{last})^2 + q_{\mathcal{T}}\mathcal{T}^2, \tag{17}$$

Algorithm 1 Proactive strategic collision avoidance scheme

for $j = 1$ **to** n_O **do**
  compute the share of responsibility $\alpha_{t,A|O_j}$ using (6)
  construct $DRVO_{A|O_j}(\alpha_{t,A|O_j})$, see Definition 3.1
  construct the COLREGs set $\mathcal{V}_{A|O_j}$, defined in Section III-B
end for
construct the set of candidate velocities Ω_c, defined in (8)
$\ell_1^* \leftarrow \infty$
for all $\mathbf{v}_c \in \Omega_c$ **do**
  if (15) is satisfied **then**
    if (16) is satisfied **then**
      if $\ell_1(\cdot; \mathbf{v}_c) < \ell_1^*$ **then**
        $\ell_1^* \leftarrow \ell_1(\cdot; \mathbf{v}_c)$, {using (17)}
        $\mathbf{v}^* \leftarrow \mathbf{v}_c$
      end if
    end if
  end if
end for
return $\mathbf{v}^*$

where v and χ may be prioritized separately through their respective non-negative penalty weights q_v, Δq_v, q_χ, Δq_χ. We penalize deviations from the preferred speed v_A^{pref}, preferred course χ_A^{pref}, and the last applied command in speed v_A^{last} and course χ_A^{last}.

The term $q_{\mathcal{T}}\mathcal{T}^2$ is a transitional cost (see [16]), which imposes an extra penalty (with weight $q_{\mathcal{T}} \geq 0$) on velocities that lead to the termination of a COLREGs-compliant maneuver. This term prevents oscillations which may occur when the dynamics of the guidance system, e.g. Line-Of-Sight (LOS) guidance, which generates the preferred velocity, is such that χ_A^{pref} does not always point towards the ASV's next waypoint. Since the ASV aims at following a straight-line trajectory from time t_{H_d}, we simply specify the transitional cost in terms of a change in the predicted side an obstacle is supposed to pass, by comparing the obstacle's location w.r.t. the ASV at the current CPA with the location at the CPA computed using the velocity $\mathbf{v}_{cr}$ and the predicted position at time t_{H_d}. Specifically, $\mathcal{T} := \sum_{j=1}^{n_O} \mathcal{T}_j$, where

$$\mathcal{T}_j := \begin{cases} 1 & \text{if the passage side has changed} \\ 0 & \text{otherwise.} \end{cases} \tag{18}$$

Note that the transitional cost also removes the need of using hysteresis (as in e.g. [13]) to avoid oscillations due to uncertainty in the decision variables. Since we implement a simple constraint set, instead of a (possibly complicated) penalty function for collision risk and COLREGs assessment, tuning the cost function becomes a straightforward task of specifying a desired maneuvering behavior for the ASV.

The resulting strategic proactive collision avoidance scheme is outlined in Algorithm 1. In case Ω_{cr} is empty, we simply omit obstacles beyond a predefined range and repeat only the affected procedures in Algorithm 1.

V. Simulation Results

A. Test setup and objectives

We demonstrate the properties of the DRVO strategy through a comparative study including RVO and VO. The

TABLE I: Initial values and limits for α_t in $DRVO$, adapted for each obstacle depending on the COLREGs scenario: head-on (HO), crossing from starboard (CRG-SB) or port (CRG-P), overtaking (OTG), and being overtaken (OT). The arrow ($\rightarrow$) denotes adaptation using (6) and Def. 3.2, and red ($\rightarrow$) means strict adaptation according to Def. 3.3.

Decision option	**Range [m]**	**HO**	**OTG/CRG-SB**	**OT/CRG-P**
Proactive (permitted)	>1000	$\alpha_0=0\rightarrow0.3$	$\alpha_0=0\rightarrow0.5$	$\alpha_0=0$
Proactive (required)	<1000	$\alpha_{-1}\rightarrow0.5$	$\alpha_{-1}\rightarrow1.0$	$\alpha_{-1}\rightarrow0.1$
Reactive (permitted)	<600	$\alpha_{-1}\rightarrow1.0$	$\alpha_{-1}\rightarrow1.0$	$\alpha_{-1}\rightarrow1.0$

main focus of the simulations is to show the effect of proactively adapting the collision avoidance strategy according to the proposals in this paper. Therefore, the particular choice of ASV model and tuning parameters is not relevant to the behavior properties discussed in this section. Algorithm 1 is implemented using C++ and used in the ROS simulation environment. We use the same implementation for all three approaches, and we simply set the α_t parameter in $DRVO(\alpha_t)$ to fixed values for RVO and VO. That is, $VO=DRVO(\alpha_t=1)$ and $RVO=DRVO(\alpha_t=0.5)$, whereas α_t is adapted for the proposed DRVO strategy with initial values α_0 selected based on COLREGs requirements for a given scenario (see Table I). All other parameters are the same for all three approaches. We use a LOS guidance law (see e.g. [14]) to generate the ASV's preferred velocity towards its planned path.

We focus on the situation where the obstacle type and intention are unknown to the ASV. The obstacle's future behavior is therefore highly uncertain and no prior knowledge (or initial prediction) of the obstacle's behavior is available. The ASV knows its own state and only the current position and course of each obstacle. We consider realistic situations at sea where deliberate decisions are expected from the ASV, more than 1 nautical mile (NM) away from an obstacle, and a CPA of 0.1 NM (i.e. 185.2m) is specified. Distances specified in Table I are used to determine when proactive and reactive actions are permitted or required (cf. COLREGs stages discussed in [2]).

B. Behavior properties in single-obstacle scenarios

The results of three different cases of a head-on scenario are presented in Fig. 4–5, where both the ASV and obstacle have the same preferred speed of 5 m/s (∼10 knots). The ASV observes the obstacle's action relative to its own action. That is, no action occurs, or the obstacle's action occurs either later, earlier, or at the same time as the ASV's action. In Fig. 4a, the obstacle acts late, but with the intention to cooperate. The VO approach simply assumes the obstacle will follow its new path, and therefore the ASV can return to its original path, as quickly as possible. The RVO approach expects the obstacle to reciprocate the ASV's actions, and since it is not the case, it also allows the ASV to return to its original path, but not as quickly as VO. The DRVO strategy evaluates the obstacle's action according to Def.

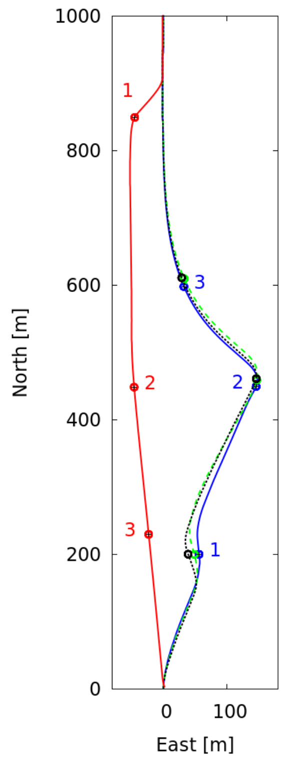

(a) Obstacle acts late.

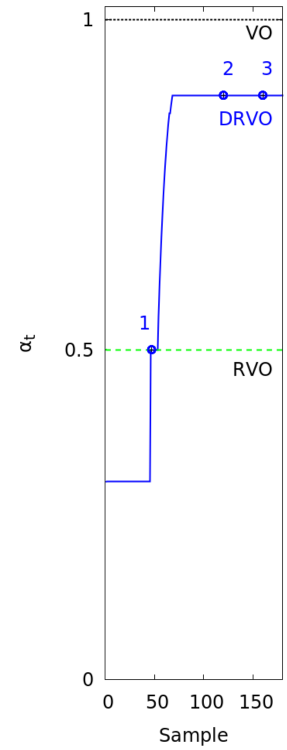

(b) α_t values (cf. (6)).

Fig. 4: Simulation of different behavior cases in a head-on scenario, showing the properties of DRVO (blue), RVO (green, dashed), and VO (black, dotted) for the ASV. The obstacle (red) is moving from North to South, and the locations 1, 2, and 3, indicate the positions of the obstacle and the ASV at the same sampling time.

3.2, and since the obstacle is cooperating, the responsibility parameter α_t is not adapted until the obstacle starts steering towards the ASV at location 1 (cf. Fig. 4a and 4b). Note that keeping α_t constant until location 1 is not the same as simply keeping a constant course or speed. Moreover, tuning a collision avoidance algorithm to keep its decisions constant for more than 100 m may not be feasible in some scenarios.

The main issue is that VO, RVO, and any other approach that does not capture the intention of the obstacle to cooperate may interpret a cooperative behavior as a change/end of a scenario. Consequently, the ASVs behavior may become reactive, unpredictable, violating COLREGs and increasing the risk of collision. In the case shown in Fig. 4a, the ASV has enough time to achieve the required CPA distance for all approaches, even though the obstacle does not take its required share of responsibility.

In Fig. 5a, the obstacle acts early, and it can be seen that all three approaches make similar decisions in the beginning. However, the decision to steer towards the original path occurs early for VO, followed by RVO, and then DRVO, which takes a more careful approach, as seen in the snap shot in the top right corner of Fig. 5a. In the case where the obstacle performs no action, as shown in Fig. 5b, the idea of encouraging the obstacle to cooperate is evident in

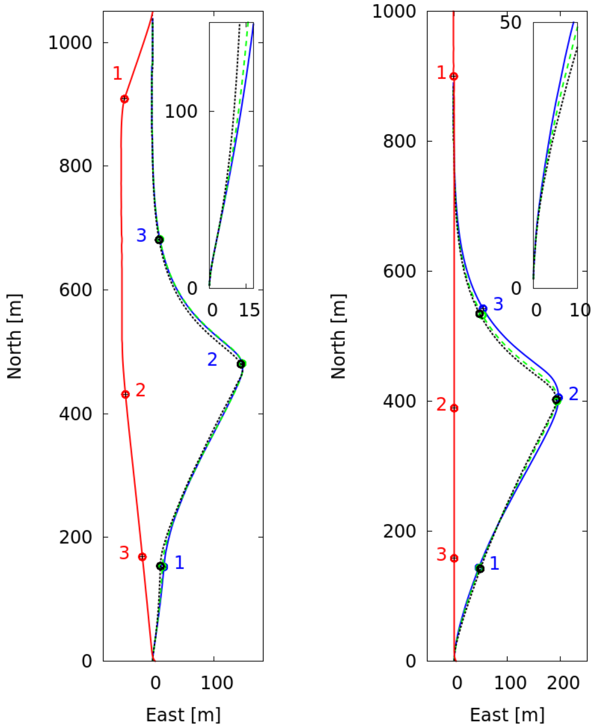

(a) Obstacle acts early.

(b) Obstacle stays on.

Fig. 5: Simulation of different behavior cases in a head-on scenario (cf. Fig. 4).

the ASV's initial behavior (see snap shot in the top right corner). DRVO begins with a much less responsibility and adapts towards full responsibility as it gets more apparent that the obstacle is not cooperating (cf. column 2 of Table I).

C. Behavior properties in multi-obstacle scenarios

We will discuss more complex situations involving three dynamic obstacles engaging the ASV in realistic scenarios, as shown in Fig. 6. In Fig 6a, the obstacles attempt to cooperate according to COLREGs, and we consider decisions in a reactive range (see Table I) since both VO and RVO are designed to perform best as reactive methods.

It can be seen in Fig. 6a that although the initial DRVO behavior coincides with RVO, the assessment of the obstacle's cooperative behavior makes it possible for DRVO to make proactive decisions by not quickly steering towards the ASVs original path when the obstacles appear to be moving out of its way (compare the location of the ASV and the obstacles at p_2). At p_2 the ASV keeps the CPA distance when using either VO, RVO, or DRVO. However, when obstacle 1 changes its course towards South, dangerous decisions are made by both VO and RVO. Both strategies allow the ASV to continue on its current course for a while since the turning maneuver of obstacle 1 still appears to move away from the ASV. This dangerous decision makes the ASV violate the specified CPA distance (185.2 m) and had to resort to an evasive maneuver, which is clearly visible for VO and less dramatic for RVO. DRVO, on the other hand, gains from the effect of its earlier

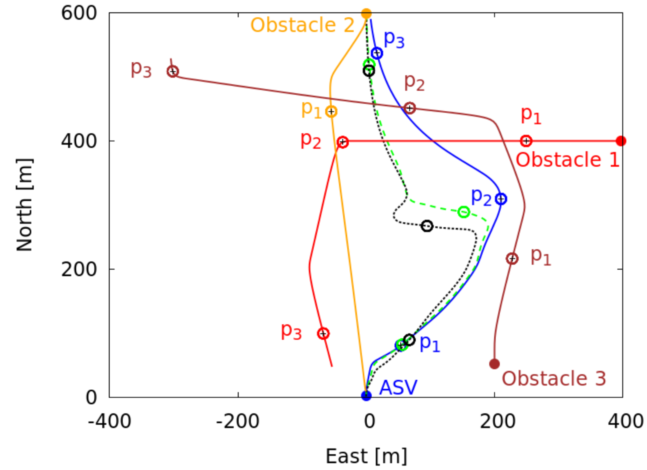

(a) Obstacles attempt to cooperate in a predictable manner.

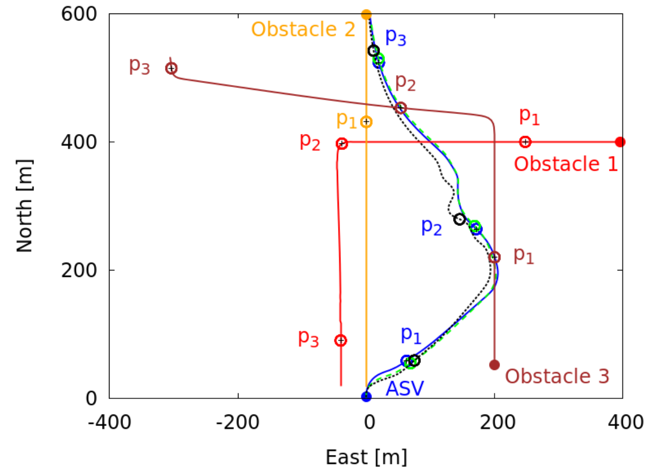

(b) Obstacles stay on their original planned paths.

Fig. 6: Simulation of different behavior cases involving head-on, crossing and overtaking scenarios. Different behaviors are recorded for the ASV using DRVO (blue), RVO (green), and VO (black). The locations p_1, p_2, and p_3, indicate the positions of the obstacles and the ASV at the same sampling time. In (b) the DRVO and RVO behaviors are almost the same.

proactive decisions and also interprets the current behavior of obstacle 1 as cooperating, and therefore does not make the dangerous situation worse.

Comparing the observations in Fig 6a with Fig. 6b, where the obstacles keep their planned paths, it becomes clear that both VO and RVO perform better when the obstacles do not cooperate. In fact, all approaches fulfill the required CPA distance, even though VO's decisions become unpredictable and DRVO's decisions are almost the same as that of RVO. Recall that RVO is designed to perform well when the cooperative behavior of the obstacles (exactly) reciprocates the ASVs own actions, a case which is hardly true at sea.

VI. Conclusions

A proactive collision avoidance method has been presented and discussed in this paper. The method extends the RVO approach with COLREGs-compliant behaviors, by taking into account the required cooperative behavior of marine vessels, which may not accurately reciprocate the behavior of other vessels. A strategy for assessing the cooperative behavior of obstacles is proposed and used in the decision process to ensure that obstacles that intend to cooperate do not lead to reactive ASV actions that increase the risk of collision.

Properties that relate the velocity obstacles framework to existing CPA techniques used for avoiding collision at sea are also discussed. A predictive approach to solving the feasibility issues of the VO framework, considering the ASV's dynamics and constraints, is proposed, and we have shown that the VO framework can be extended to include more refined objectives suitable for ASVs.

The simulation results show that the proposed DRVO method performs better than both VO and RVO when obstacles cooperate by following COLREGs. Moreover the results provide a step towards achieving more realistic and predictable ASV behavior in complex situations at sea that are typically resolved by required cooperative actions. Further work will include experiments and a study on the effect of uncertain decision variables and unknown disturbances.

VII. APPENDIX

A. Proof of Proposition 2.1

We show that d_{AB}^{CPA} is equal to radius $r\left(\mathbf{p}_B, \boldsymbol{\lambda}(\mathbf{p}_A, \mathbf{v}_{A|B})\right)$ in (i) using Fig. 7. Consider the ray $\boldsymbol{\lambda}(\mathbf{p}_B, \mathbf{v}_{A|B}^{\perp})$ from $\mathbf{p}_B$ in the direction perpendicular to the relative velocity $\mathbf{v}_{A|B}$. The intersection $\mathbf{p}_I$ of $\boldsymbol{\lambda}(\mathbf{p}_B, \mathbf{v}_{A|B}^{\perp})$ and $\boldsymbol{\lambda}(\mathbf{p}_A, \mathbf{v}_{A|B})$ is a tangent point of a circle centered at $\mathbf{p}_B$ with radius $r\left(\mathbf{p}_B, \boldsymbol{\lambda}(\mathbf{p}_A, \mathbf{v}_{A|B})\right)$ shown in Fig. 7. The following derivation shows that the time at the intersection is the t_{AB}^{CPA} given by (2), which is used to obtain the d_{AB}^{CPA} in (3):

$$\boldsymbol{\lambda}(\mathbf{p}_A, \mathbf{v}_{A|B}) = \boldsymbol{\lambda}(\mathbf{p}_B, \mathbf{v}_{A|B}^{\perp}) \Rightarrow \mathbf{p}_A + t\mathbf{v}_{A|B} = \mathbf{p}_B + t\mathbf{v}_{A|B}^{\perp}$$
$$t = \frac{\mathbf{p}_{BA} \cdot \mathbf{v}_{A|B}}{(\mathbf{v}_{A|B} - \mathbf{v}_{A|B}^{\perp}) \cdot \mathbf{v}_{A|B}} = \frac{\mathbf{p}_{BA} \cdot \mathbf{v}_{A|B}}{\|\mathbf{v}_{A|B}\|^2}$$

which defines the t_{AB}^{CPA} in (2). Using Fig. 7, we can obtain an expression for the radius as (cf. (3)):

$$\begin{aligned} r\left(\mathbf{p}_B, \boldsymbol{\lambda}(\mathbf{p}_A, \mathbf{v}_{A|B})\right) &= \|\mathbf{p}_I - \mathbf{p}_B\| \\ &= \|(\mathbf{p}_I - \mathbf{p}_A) - (\mathbf{p}_B - \mathbf{p}_A)\| \\ &= \|t_{AB}^{\mathrm{CPA}}(\mathbf{v}_A - \mathbf{v}_B) - \mathbf{p}_B + \mathbf{p}_A\| = d_{AB}^{\mathrm{CPA}}. \end{aligned}$$

The necessary and sufficient conditions in (ii) follow from the result in (i) using $r\left(\mathbf{p}_B, \boldsymbol{\lambda}(\mathbf{p}_A, \mathbf{v}_{A|B})\right) = d_{AB}^{min}$ and Lemma 1 in [5]. Moreover, at the closest point of approach, A's velocity $\mathbf{v}_A$ is tangent to the circle of radius $r\left(\mathbf{p}_B, \boldsymbol{\lambda}(\mathbf{p}_A, \mathbf{v}_{A|B})\right) = d_{AB}^{min}$ around B, and can therefore neither yield $d_{AB}^{\mathrm{CPA}} < d_{AB}^{min}$ nor $d_{AB}^{\mathrm{CPA}} > d_{AB}^{min}$.

Finally, consider the size and shape of A and B expanded as circles such that $r_A + r_B = r\left(\mathbf{p}_B, \boldsymbol{\lambda}(\mathbf{p}_A, \mathbf{v}_{A|B})\right)$. This implies $\boldsymbol{\lambda}(\mathbf{p}_A, \mathbf{v}_{A|B})$ is a tangent to the circle describing the boundary of the set $\mathcal{B} \oplus -\mathcal{A}$ (cf. Def. 2.1). Therefore, $\boldsymbol{\lambda}(\mathbf{p}_A, \mathbf{v}_{A|B})$ corresponds to an edge of $CC_{A|B}$. The other edge is the reflection of $\boldsymbol{\lambda}(\mathbf{p}_A, \mathbf{v}_{A|B})$ about $\mathbf{p}_{BA}$, which completes the proof.

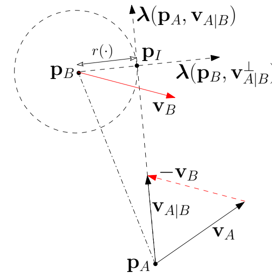

Fig. 7: Illustration for deriving $d_{AB}^{\mathrm{CPA}} = r\left(\mathbf{p}_B, \boldsymbol{\lambda}(\mathbf{p}_A, \mathbf{v}_{A|B})\right)$.

REFERENCES

[1] IMO, "Convention on the International Regulations for Preventing Collisions at Sea, (COLREGs)," 1972. [Online]. Available: http://www.imo.org/en/About/conventions/listofconventions/pages/colreg.aspx

[2] A. Cockcroft and J. Lameijer, "Part B - Steering and sailing rules," in *A Guide to the Collision Avoidance Rules (Seventh Edition)*, seventh edition ed. Oxford: Butterworth-Heinemann, 2012, pp. 11 – 104.

[3] J. van den Berg, M. Lin, and D. Manocha, "Reciprocal Velocity Obstacles for real-time multi-agent navigation," in *2008 IEEE International Conference on Robotics and Automation*, May 2008, pp. 1928–1935.

[4] B. Kluge and E. Prassler, "Reflective navigation: individual behaviors and group behaviors," in *2004 IEEE International Conference on Robotics and Automation*, vol. 4, April 2004, pp. 4172–4177.

[5] P. Fiorini and Z. Shiller, "Motion Planning in Dynamic Environments Using Velocity Obstacles," *The International Journal of Robotics Research*, vol. 17, no. 7, pp. 760–772, 1998.

[6] D. Wilkie, J. van den Berg, and D. Manocha, "Generalized velocity obstacles," in *2009 IEEE/RSJ International Conference on Intelligent Robots and Systems*, Oct 2009, pp. 5573–5578.

[7] D. Bareiss and J. van den Berg, "Generalized Reciprocal Collision Avoidance," *Int. J. Rob. Res.*, vol. 34, no. 12, pp. 1501–1514, 2015.

[8] D. Fox, W. Burgard, and S. Thrun, "The dynamic window approach to collision avoidance," *IEEE Robotics Automation Magazine*, vol. 4, no. 1, pp. 23–33, Mar 1997.

[9] L. Martinez-Gomez and T. Fraichard, "Collision Avoidance in Dynamic Environments: An ICS-based Solution and Its Comparative Evaluation," in *2009 IEEE International Conference on Robotics and Automation*, Piscataway, NJ, USA, 2009, pp. 2251–2256.

[10] T. A. Johansen, T. Perez, and A. Cristofaro, "Ship Collision Avoidance and COLREGS Compliance Using Simulation-Based Control Behavior Selection With Predictive Hazard Assessment," *IEEE Transactions on Intelligent Transportation Systems*, vol. 17, no. 12, pp. 3407–3422, Dec 2016.

[11] B. O. H. Eriksen and M. Breivik, "MPC-Based Mid-level Collision Avoidance for ASVs using Nonlinear Programming," in *2017 IEEE Conference on Control Technology and Applications (CCTA)*, Aug 2017, pp. 766–772.

[12] J. Snape, J. v. d. Berg, S. J. Guy, and D. Manocha, "The Hybrid Reciprocal Velocity Obstacle," *IEEE Transactions on Robotics*, vol. 27, no. 4, pp. 696–706, Aug 2011.

[13] Y. Kuwata, M. T. Wolf, D. Zarzhitsky, and T. L. Huntsberger, "Safe Maritime Autonomous Navigation With COLREGS, Using Velocity Obstacles," *IEEE Journal of Oceanic Engineering*, vol. 39, no. 1, pp. 110–119, Jan 2014.

[14] T. I. Fossen, *Handbook of Marine Craft Hydrodynamics and Motion Control*. John Wiley & Sons, Ltd, 2011.

[15] S. J. Guy, J. Chhugani, C. Kim, N. Satish, M. Lin, D. Manocha, and P. Dubey, "ClearPath: Highly Parallel Collision Avoidance for Multi-agent Simulation," in *Proceedings of the 2009 ACM SIGGRAPH/Eurographics Symposium on Computer Animation*, ser. SCA '09. New York, NY, USA: ACM, 2009, pp. 177–187.

[16] I. B. Hagen, D. K. M. Kufoalor, E. F. Brekke, and T. A. Johansen, "MPC-based Collision Avoidance Strategy for Existing Marine Vessel Guidance Systems," in *Proceedings of the 2018 IEEE International Conference on Robotics and Automation*, Brisbane, Australia, 2018.